The solution of Lanchester's equations with inter-battle reinforcement strategies

Mark McCartney

Faculty of Computing, Engineering & Built Environment

Ulster University

Newtownabbey

Northern Ireland

m.mccartney@ulster.ac.uk

Abstract

A two-army conflict made up of repeated battles with inter-battle reinforcements is considered. Each battle is modelled via Lanchester's 'aimed fire' model and three reinforcement strategies; constant, and linearly and quadratically varying (with respect to post-battle troop levels) are investigated. It is shown that while a constant reinforcement strategy will always lead to an outright victory via a simple partitioning of the two dimensional army strength space, linear reinforcement can lead to stalemate, and quadratically varying reinforcement can lead to stalemate, with quasi-periodic and chaotic behaviour, and the creation of fractal partitioning of the army strength space.

Introduction

Lanchester's equations[1] form a very simple mathematical model for warfare and have been applied to the study of historic battles[2] including the 1994-45 Battle of the Bulge[3], the 1940 Battle of Britain[4], and the 1916 Battle of Jutland[5]. They have also been applied in other contexts including combat in the animal kingdom[6] and human evolution[7]. While Lanchester's work was arrived independently and almost simultaneously by Osipov[8], we will continue with the tradition of describing the mathematical model using Lanchester's name.

Lanchester's equations take two forms. Let us consider two sides, Red and Green, who have forces of size R(t) and G(t) respectively. Lanchester's 'unaimed fire' model is of the form

$$\begin{aligned} \frac{dG}{dt} &= -\gamma GR \\ \frac{dR}{dt} &= -\delta GR \end{aligned} \quad . \tag{1}$$

In this model the attrition rate of one force is proportional to both its size and the size of the opponent, with γ and δ being the rate of fire per combatant of Red and Green respectively. This model can be thought of in terms of the attacking force firing in an unaimed or random way, with the probability of a resulting kill thus being proportional to the size of the opponent's army, who it is assumed do not regroup to maintain a constant troop density on the battle field. Such modelling is appropriate for use of artillery against infantry, where artillery shells will destroy everything within a given area, and thus the attrition rate will be proportional to the number of soldiers per unit area.

The second form of Lanchester's equations is the 'aimed fire' model

$$\begin{aligned} \frac{dG}{dt} &= -\alpha R \\ \frac{dR}{dt} &= -\beta G \end{aligned} \tag{2}$$

where α and β are the number of kills per unit time that each combatant in R and G inflict.

These models can of course be combined to form a linear sum of aimed and unaimed fire components[9] and extended to a generalised power law[3],

$$\begin{aligned} \frac{dG}{dt} &= -AR^p G^q \\ \frac{dR}{dt} &= -BR^q G^p \end{aligned} \quad . \tag{3}$$

In what follows in this paper we will focus solely on the aimed fire model (2) with the novel feature of considering it as the basis for repeated fixed time period battles with a range in inter-battle reinforcement strategies.

Lanchester's 'aimed fire' model

Given initial troop levels R_0 and G_0 the aimed fire model (2) can be solved explicitly to give

$$G = G_0 \cosh\left(\sqrt{\alpha\beta}t\right) - \sqrt{\frac{\alpha}{\beta}} R_0 \sinh\left(\sqrt{\alpha\beta}t\right)$$
$$R = R_0 \cosh\left(\sqrt{\alpha\beta}t\right) - \sqrt{\frac{\beta}{\alpha}} G_0 \sinh\left(\sqrt{\alpha\beta}t\right) \quad (4)$$

With the time to the end of the battle being given by

$$T_\Omega = \frac{1}{2\sqrt{\alpha\beta}} \ln\left|\frac{\sqrt{\alpha}R_0 + \sqrt{\beta}G_0}{\sqrt{\alpha}R_0 - \sqrt{\beta}G_0}\right| \quad (5)$$

where if

$$\begin{aligned} \beta G_0^2 - \alpha R_0^2 &> 0 \quad \text{Green wins} \\ \beta G_0^2 - \alpha R_0^2 &< 0 \quad \text{Red wins} \\ \beta G_0^2 - \alpha R_0^2 &= 0 \quad \text{mutual destruction.} \end{aligned} \quad (6)$$

In this last case of ‘mutual destruction’ the time to the conclusion of the battle diverges.

We note in pasting that form of (6) gives rise to an alternative title for the aimed fire model, namely Lanchester’s law of squares, as assuming a battle continues until an outright victory, the overall winner is determined solely by the squares of the sizes of the forces along with the kill rates.

Constant Inter-battle Reinforcement

A variant of this model is to assume that instead of a single battle there are a sequence of repeated battles in between which reinforcement s are added to each side. We will call this set of battles the *conflict* and we say that the conflict has ended if at the end of a given battle one side’s forces are exhausted before reinforcement s can be added. We shall assume that each battle lasts a time $\tau < T_\Omega$, otherwise the conflict will be concluded at the first battle. If we write the level of Green and Red forces at the beginning of the (i+1)th battle to be $\underline{A}_i = \begin{bmatrix} G_i \\ R_i \end{bmatrix}$ then

$$\underline{A}_{i+1} = K\underline{A}_i + \underline{\Re}^C \quad (7)$$

where $\underline{\Re}^C = \begin{bmatrix} G^R \\ R^R \end{bmatrix}$ and R^R and G^R are constant reinforcement levels which are added to Red and Green at the beginning of each new battle. Further, what we will call the kill matrix, *K*, is of the form.

$$K = \begin{bmatrix} \cosh\left(\sqrt{\alpha\beta}\tau\right) & -\sqrt{\frac{\alpha}{\beta}} \sinh\left(\sqrt{\alpha\beta}\tau\right) \\ -\sqrt{\frac{\beta}{\alpha}} \sinh\left(\sqrt{\alpha\beta}\tau\right) & \cosh\left(\sqrt{\alpha\beta}\tau\right) \end{bmatrix}. \quad (8)$$

The eigenvalues and eigenvectors of *K* are

$$\lambda = \exp\left(\pm\sqrt{\alpha\beta}\tau\right) \quad (9)$$

and

$$\underline{e} = \begin{bmatrix} 1 \\ \mp\sqrt{\dfrac{\beta}{\alpha}} \end{bmatrix}. \tag{10}$$

The fixed point of (7) can be shown to be,

$$A^* = \begin{bmatrix} \dfrac{1}{2}\left(G^R + \sqrt{\dfrac{\alpha}{\beta}} R^R \coth\left(\dfrac{1}{2}\sqrt{\alpha\beta}\tau \right)\right) \\ \dfrac{1}{2}\left(R^R + \sqrt{\dfrac{\beta}{\alpha}} G^R \coth\left(\dfrac{1}{2}\sqrt{\alpha\beta}\tau \right)\right) \end{bmatrix} \tag{11}$$

and the form of the eigenvalues (9) means that we have a saddle point at A^* with separatrices

$$G = \pm\sqrt{\frac{\alpha}{\beta}} R + \frac{1}{2}\left(G^R \mp \sqrt{\frac{\alpha}{\beta}} R^R \right)\left(1 \mp \coth\left(\frac{1}{2}\sqrt{\alpha\beta}\tau \right)\right). \tag{12}$$

The overall form of the solution of this system is illustrated in Figure 1. The representative trajectories drawn are solutions to (7). Trajectories entering the grey and light grey regions indicate the last battle in the conflict, by the end of which Red (light grey region) or Green (grey region) will have won an outright victory before further reinforcement s can arrive. The separatrix S1 in Figure 1 divides (R,G) into two regions. In the region above S1, Green wins, and in the region below Red wins.

Figure 1 provides commanders with strategy diagram. Thus, for example, if the commander of the Green forces determines that he is on the bottom quadrant and is destined for defeat then if he can add, as a one off, a significant enough level of reinforcement s before the next battle to move his army into the left quadrant then Green will ultimately win. This of course assumes that Red does not change her strategy. Further, the earlier Green does this the less forces he will have to add to move quadrant and change the overall outcome. This means that if a relatively small number extra reserve troops are added early on, they may tip the battle. This is more likely to succeed if the opponent does not notice this change until the one-off troop change that she would have to introduce to move quadrant is beyond her reserve capabilities.

Linearly Variable Inter-battle Reinforcement

A more realistic model is to make the reinforcement level a function of the number of troops remaining after the previous battle (ie a function of $G_i \cosh\left(\sqrt{\alpha\beta}\tau\right) - \sqrt{\frac{\alpha}{\beta}} R_i \sinh\left(\sqrt{\alpha\beta}\tau\right)$ for Green and of $R_i \cosh\left(\sqrt{\alpha\beta}\tau\right) - \sqrt{\frac{\beta}{\alpha}} G_i \sinh\left(\sqrt{\alpha\beta}\tau\right)$ for Red). We expect this functional form to be such that the reinforcement s will be large when the number of troops remaining after the last battle is small, and to decrease with increasing soldier levels. A simple linear functional forms for Green and Red reinforcement s is given by

$$\underline{A}_{i+1} = K\underline{A}_i + \underline{\Re}^L \tag{13}$$

where

$$\underline{\Re}^L = \begin{bmatrix} G^R\left(1-\frac{1}{\gamma}\left(G_i\cosh\left(\sqrt{\alpha\beta}\tau\right)-\sqrt{\frac{\alpha}{\beta}}R_i\sinh\left(\sqrt{\alpha\beta}\tau\right)\right)\right) \\ R^R\left(1-\frac{1}{\delta}\left(R_i\cosh\left(\sqrt{\alpha\beta}\tau\right)-\sqrt{\frac{\beta}{\alpha}}G_i\sinh\left(\sqrt{\alpha\beta}\tau\right)\right)\right) \end{bmatrix}. \tag{14}$$

Where G^R and R^R are the maximum reinforcement levels for Green and Red and γ and δ are soldier level scalings (assumed to be greater than G^R and R^R) above which instead of reinforcement s being added to the battlefield they are instead removed . This troop removal scenario will not occur provided initial troop levels for Green and Red are assumed to be less than γ and δ respectively.

This leads directly to a model of the form

$$\underline{A}_{i+1} = L\underline{A}_i + \underline{\Re}^C \tag{15}$$

where

$$L = \begin{bmatrix} \left(1-\frac{G_R}{\gamma}\right)\cosh\left(\sqrt{\alpha\beta}\tau\right) & -\left(1-\frac{G_R}{\gamma}\right)\sqrt{\frac{\alpha}{\beta}}\sinh\left(\sqrt{\alpha\beta}\tau\right) \\ -\left(1-\frac{R_R}{\delta}\right)\sqrt{\frac{\beta}{\alpha}}\sinh\left(\sqrt{\alpha\beta}\tau\right) & \left(1-\frac{R_R}{\delta}\right)\cosh\left(\sqrt{\alpha\beta}\tau\right) \end{bmatrix}. \tag{16}$$

While mathematically the overall form of (15) is the same as (7) the significant difference is that if

$$\cosh\left(\sqrt{\alpha\beta}\tau\right) < \frac{1+\left(1-\frac{G^R}{\gamma}\right)\left(1-\frac{R^R}{\delta}\right)}{\left(1-\frac{G^R}{\gamma}\right)+\left(1-\frac{R^R}{\delta}\right)} \tag{17}$$

both eigenvalues of L will be less than unity and hence the fixed point will be stable. While the fixed point and equations of the separatrices can be written down in general terms for (15) they are unwieldy and instead we will give solutions for the restricted case where both Red and Green adopt the same reinforcement strategy where

$$\left(1-\frac{G^R}{\gamma}\right) = \left(1-\frac{R^R}{\delta}\right) = f\ . \tag{18}$$

In this case

$$L = fK \tag{19}$$

and the eigenvalues and eigenvectors of L are given by

$$\lambda = f\exp\left(\pm\sqrt{\alpha\beta}\tau\right) \tag{20}$$

and (10) respectively. The fixed point is given by

$$A^* = \begin{bmatrix} \dfrac{R^R\sqrt{\dfrac{\alpha}{\beta}} f \sinh\left(\sqrt{\alpha\beta}\tau\right) + G^R\left(f\cosh(\sqrt{\alpha\beta}\tau) - 1\right)}{2f\cosh(\sqrt{\alpha\beta}\tau) - 1 - f^2} \\ \dfrac{G^R\sqrt{\dfrac{\beta}{\alpha}} f \sinh\left(\sqrt{\alpha\beta}\tau\right) + R^R\left(f\cosh(\sqrt{\alpha\beta}\tau) - 1\right)}{2f\cosh(\sqrt{\alpha\beta}\tau) - 1 - f^2} \end{bmatrix}. \qquad (21)$$

which is stable provided,

$$\sqrt{\alpha\beta}\tau < -\ln f \qquad (22)$$

and the separatrices are

$$G = \pm\sqrt{\frac{\alpha}{\beta}}R + \left(G^R \mp \sqrt{\frac{\alpha}{\beta}}R^R\right)\left(\frac{f\exp\left(\mp\sqrt{\alpha\beta}\tau\right) - 1}{2f\cosh\left(\sqrt{\alpha\beta}\tau\right) - 1 - f^2}\right). \qquad (23)$$

If, as illustrated in Figure 2, inequality (22) holds and the fixed point is stable then the conflict will reach a stalemate, with each side repeatedly adding reinforcement s but failing to reach victory. In such a case to achieve an overall conflict victory Green (Red) needs to attempt to move the fixed point into the grey (light grey) region of Figure 2. Thus, Red can ensure victory if they can increase their maximum reinforcement levels G^R to

$$R^R \geq \sqrt{\frac{\beta}{\alpha}}\left(\frac{\cosh\left(\sqrt{\alpha\beta}\tau\right) - f}{\sinh\left(\sqrt{\alpha\beta}\tau\right)}\right)G^R \qquad (24)$$

and similarly, Green can ensure victory if

$$G^R \geq \sqrt{\frac{\alpha}{\beta}}\left(\frac{\cosh\left(\sqrt{\alpha\beta}\tau\right) - f}{\sinh\left(\sqrt{\alpha\beta}\tau\right)}\right)R^R \ . \qquad (25)$$

Quadratically Variable Inter-battle Reinforcement s

A final model is to make the reinforcement levels vary quadratically with the number of soldiers remaining after the previous battle:

$$\underline{A}_{i+1} = K\underline{A}_i + \underline{\Re}^Q \qquad (26)$$

where

$$\underline{\mathfrak{R}}^{Q}=\begin{bmatrix}\frac{4G^{R}}{\gamma}\left(G_i\cosh\left(\sqrt{\alpha\beta}\tau\right)-\sqrt{\frac{\alpha}{\beta}}R_i\sinh\left(\sqrt{\alpha\beta}\tau\right)\right)\left(1-\frac{1}{\gamma}\left(G_i\cosh\left(\sqrt{\alpha\beta}\tau\right)-\sqrt{\frac{\alpha}{\beta}}R_i\sinh\left(\sqrt{\alpha\beta}\tau\right)\right)\right)\\ \frac{4R^{R}}{\delta}\left(R_i\cosh\left(\sqrt{\alpha\beta}\tau\right)-\sqrt{\frac{\beta}{\alpha}}G_i\sinh\left(\sqrt{\alpha\beta}\tau\right)\right)\left(1-\frac{1}{\delta}\left(R_i\cosh\left(\sqrt{\alpha\beta}\tau\right)-\sqrt{\frac{\beta}{\alpha}}G_i\sinh\left(\sqrt{\alpha\beta}\tau\right)\right)\right)\end{bmatrix}. \tag{27}$$

In this model, maximum reinforcement levels for Green (Red) will be G^R (R^R) and will occur when the troop levels are *γ/2* (*δ/2*) respectively. Around these peaks reinforcement levels will decrease as post battle troop levels increase (as with the linear reinforcement model), but they will also decrease as post battle troop levels decrease. This latter scenario means that for low post-battle troop levels the commander may in effect be considering conceding the conflict.

The system (26) can be transformed to a pair of linearly coupled logistic maps. However, it is more convenient to leave the system expressed in terms of scaled troop levels as

$$\begin{aligned}R'_{i+1}&=\left(R'_i\cosh\left(\sqrt{\alpha\beta}\tau\right)-\frac{1}{\xi}G'_i\sinh\left(\sqrt{\alpha\beta}\tau\right)\right)\left(1-4R'^{R}\left(R'_i\cosh\left(\sqrt{\alpha\beta}\tau\right)-\frac{1}{\xi}G'_i\sinh\left(\sqrt{\alpha\beta}\tau\right)-1\right)\right)\\ G'_{i+1}&=\left(G'_i\cosh\left(\sqrt{\alpha\beta}\tau\right)-\xi R'_i\sinh\left(\sqrt{\alpha\beta}\tau\right)\right)\left(1-4G'^{R}\left(G'_i\cosh\left(\sqrt{\alpha\beta}\tau\right)-\xi R'_i\sinh\left(\sqrt{\alpha\beta}\tau\right)-1\right)\right)\end{aligned} \tag{28}$$

where

$$\xi=\sqrt{\frac{\alpha}{\beta}}\frac{\delta}{\gamma} \tag{29}$$

and troop levels gave been scaled via

$$\begin{aligned}R'_i&=\frac{R_i}{\delta},\quad G'_i=\frac{G_i}{\gamma}\\ R'^{R}&=\frac{R^R}{\delta},\ G'^{R}=\frac{G^R}{\gamma}.\end{aligned} \tag{30}$$

In what follows we investigate the behaviour of (28) for $R'^{R}, G'^{R}\in[0,1]$ and $R'\in[0,R'^{R}], G'\in[0,G'^{R}]$.

We can think of ξ as a ‘power ratio’ of Red to Green, with the numerator (denominator) being the product of the root of the kill rate and the maximum reinforcement levels of the Red (Green) forces.

As with the constant and linearly varying reinforcement models we say that a conflict has ended if at the end of a given battle one side’s forces are exhausted before reinforcement s can be added.

Figure 3 shows a representative set of examples of regions of $\left(R', G'\right)$ space, with R' and G' scaled as fractions of R'^{R} and G'^{R}, which lead to victory for Green (grey regions); a victory for Red (light grey regions); or lead to a stalemate (white regions). In all the plots $\sqrt{\alpha\beta}\tau = \frac{1}{4}$ and $\xi = \frac{5}{4}$, and $R^{'R} = G^{'R}$. Figure 3(a-c), where $R^{'R} = G^{'R} = \frac{1}{4}, \frac{1}{2}, \frac{3}{4}$, illustrate that for small values of $R^{'R} = G^{'R}$ the model behaves in a way comparable to the constant (7) or linear (13) reinforcement model, with the $\left(R^{'}, G^{'}\right)$ space being divided into simple regions of victory or stalemate. As $R^{'R} = G^{'R}$ increase further the behaviour becomes more interesting. The region of stalemate disappears and is replaced with fractal basins of victory as shown in Figures 3(d-f). The fractal nature of these plots is illustrated in Figure 3(f) which shows a 10 factor zoom on the centre of Figure 3(e). Figures 3(g-h) give Feigenbaum diagrams for examples of the evolution of the for R' and G' as $R^{'R} = G^{'R}$ vary over the range [0,1]. The values of $R^{'R} = G^{'R}$ which do not produce an attractor are those for which, from the starting value (R'= $R^{'R}$, G'=$G^{'R}$), the system evolves to a Red or Green victory. Figures 3(i-k) give examples of attractors as $R^{'R} = R^{'G}$ increases from 0.68 to 0.71 to 0.75. In particular, 3(i), where $R^{'R} = R^{'G} = 0.68$, gives an example of the existence of a closed invariant curve evolving from the period two orbit which exists between approximately 0.58 and 0.67. In figures 3(j) and 3(k) the clear vertical and horizontal boundaries on the attractors are formed by the maxima of (28) which occur at $\frac{\left(1+4R^{'R}\right)^2}{16R^{'R}}$ and $\frac{\left(1+4G^{'R}\right)^2}{16G^{'R}}$.

Figure 3 provides a particular set of examples for the parameter choices $\sqrt{\alpha\beta}\tau = \frac{1}{4}$ and $\xi = \frac{5}{4}$ illustrating the range of behaviours which can occur. Figures 4-6 provide summary data over $\left(\xi, R^{'R} = G^{'R}\right)$ space for $\sqrt{\alpha\beta}\tau = \frac{1}{4}, \frac{1}{2}, \frac{3}{4}$. Thus Figure 3(c) is represented by one point $\left(\xi = 1.25, R^{'R} = G^{'R} = 0.75\right)$ on each of Figures 4(a-c). With the point on Figure 4(a) giving the fraction of Figure 3(c) shaded grey (Green win); Figure 4(b) the fraction of Figure 3(c) shaded light grey (Red) win: and Figure 4(c) the fraction of Figure 3(c) shaded white (stalemate). The broad trends illustrated in these figures are twofold. First the dependence of wins for Red and Green on the value of $R^{'R} = G^{'R}$, and the fraction of space that leads to stalemate, both decrease as $\sqrt{\alpha\beta}\tau$ increases. This is because as $\sqrt{\alpha\beta}\tau$ increases the region of $\left(R^{'}, G^{'}\right)$ space which leads to victory after one battle (ie before reinforcement s dependant on the value of $R^{'R} = G^{'R}$ arrive) increases as $\tanh\left(\sqrt{\alpha\beta}\tau\right)$. Secondly, and unsurprisingly, as ξ increases, and the overall 'power' of Red forces increases relative to Green forces, the fraction of victories for Red increases.

Concluding Remarks

A conflict involving repeated battles with inter-battle reinforcement s is certainly a realistic scenario in modern warfare, albeit being modelled here in an idealised way with equi-time battles and fixed reinforcement strategies. Nevertheless, these simplified models reveal a richer behaviour than the single battle Lanchester model (2) which simply divides the (R,G) force space Red (Green) victory sub-spaces above (below) the separatrix

$$G = \sqrt{\frac{\alpha}{\beta}}R. \tag{31}$$

If we move to a constant inter-battle reinforcement (7) the separatrix shifts to

$$G=\sqrt{\frac{\alpha}{\beta}}R+\frac{1}{2}\left(G^{R}-\sqrt{\frac{\alpha}{\beta}}R^{R}\right)\left(1-\coth\left(\frac{1}{2}\sqrt{\alpha\beta}\tau\right)\right). \tag{32}$$

With the addition of linearly varying inter-battle reinforcement s (13) , depending on parameter choices the space can be divided by a single separatrix

$$G=\sqrt{\frac{\alpha}{\beta}}R+\left(G^{R}-\sqrt{\frac{\alpha}{\beta}}R^{R}\right)\left(\frac{f\exp\left(-\sqrt{\alpha\beta}\tau\right)-1}{2f\cosh\left(\sqrt{\alpha\beta}\tau\right)-1-f^{2}}\right) \tag{33}$$

or, if (22) holds, can result in a stalemate.

Finally, if a quadratic reinforcement strategy is adopted a wide range of outcomes are possible. These range from the division of (R,G) space into two regions via a simple curve; to the existence of a stalemate region with periodic, quasi-periodic or chaotic attractors; to (R,G) space being divided into fractal basins. Clearly these last chaotic and fractal scenarios are results of extreme and, one hopes, unrealised strategies. But they remain an interesting example of the rich dynamics of Lanchester inspired systems.

In future work we intend to study reinforcement strategies based on estimations of both own *and* opponent troop levels, and extend to a mixed Lanchester system combining aimed and unaimed fire components.

Figures

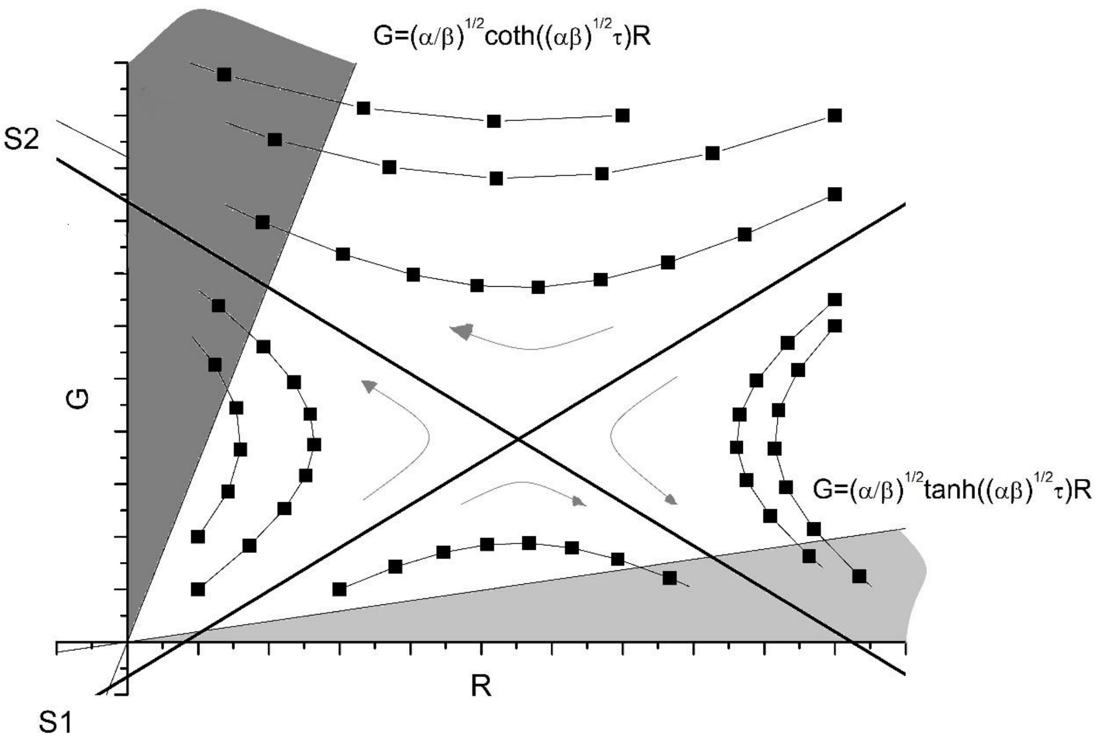

Figure 1 Phase space diagram corresponding to the constant reinforcement model (7) for

with the form of the inset S1 and outset S2 being given by (12) Once a trajectory enters the light grey region Red will win by the end of the current battle, and once a trajectory enters the grey region Green will win by the end of the current battle. Representative trajectories (squares joined with lines) are shown. The arrows indicate the direction of the trajectories under iteration.

If Green or Red forces are in the grey and light grey regions at the beginning of a battle, then by the time of the battle's conclusion Red (light grey region) or Green (grey region) will have won an outright victory before further reinforcement s arrive.

Figure 2

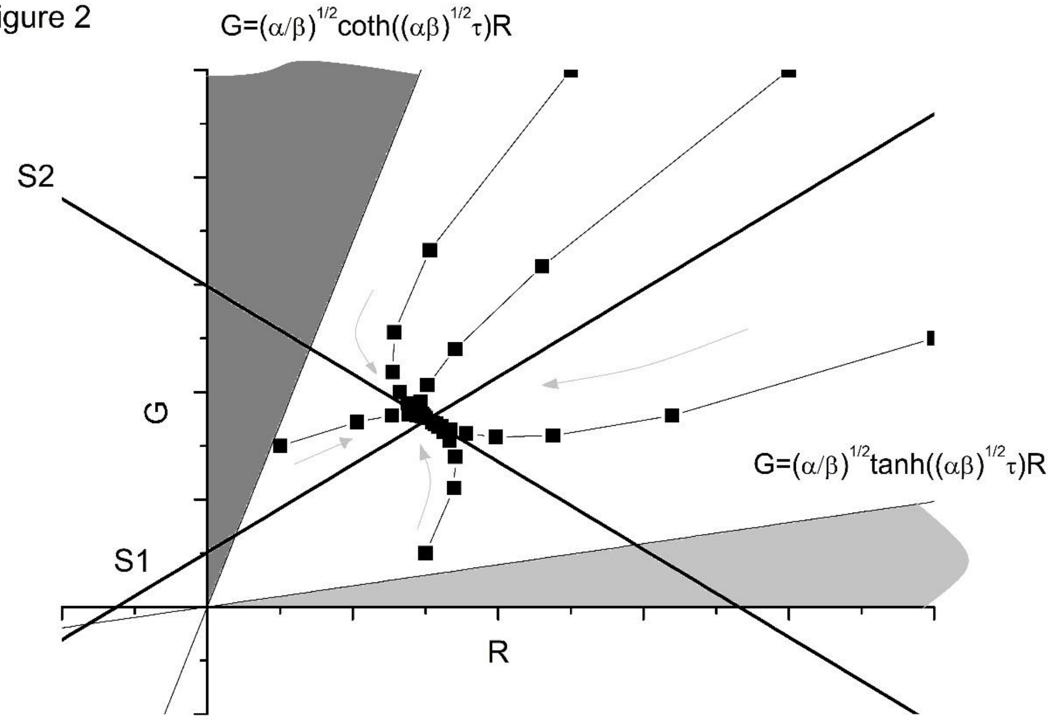

Figure 2 Phase space diagram corresponding to the linear reinforcement model (15) where inequality (22) holds and all trajectories evolve towards the stable fixed point of the model (21). The separatrices S1 and S2 are given by (23). As for figure 1, if Green or Red forces are in the grey and light grey regions at the beginning of a battle, then by the time of the battle's conclusion Red (light grey region) or Green (grey region) will have won an outright victory before further reinforcement s arrive.

Figure 3a

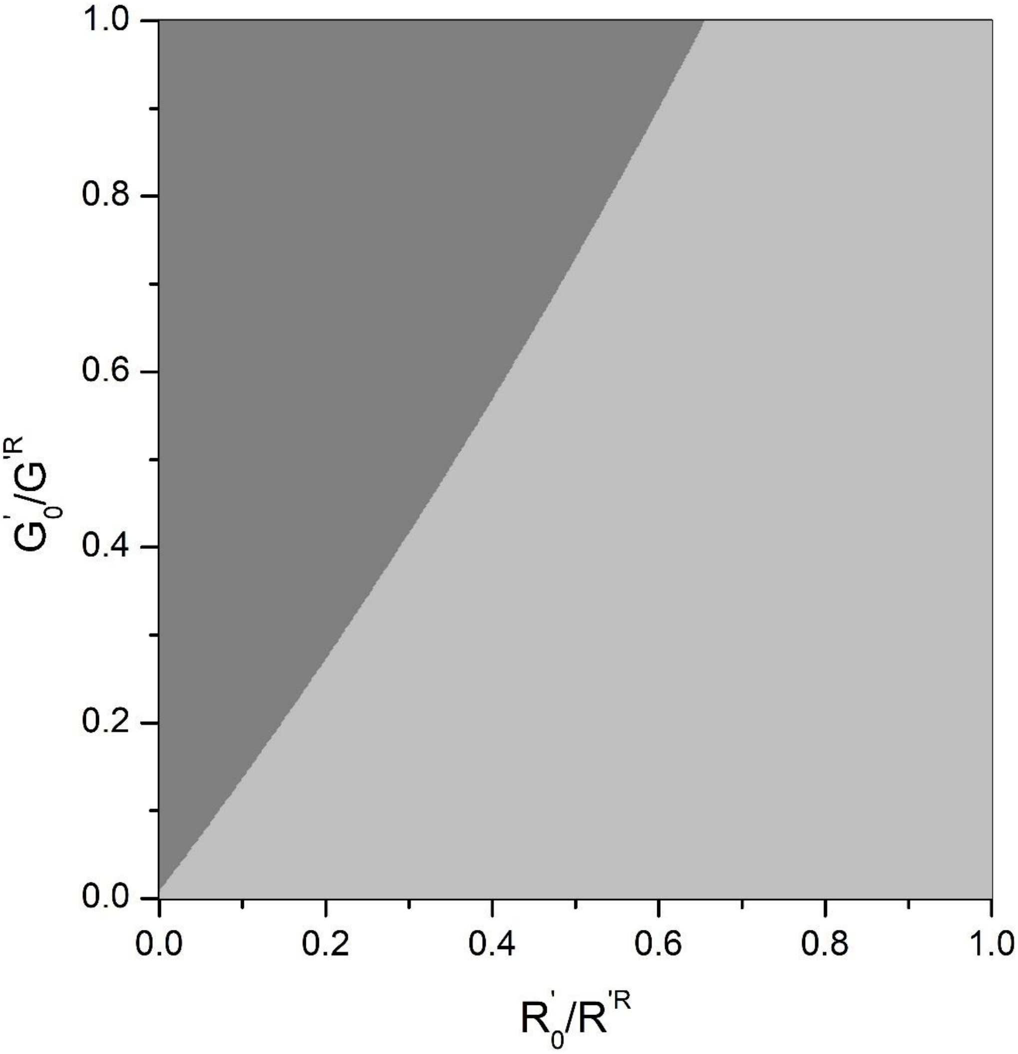

Figure 3b

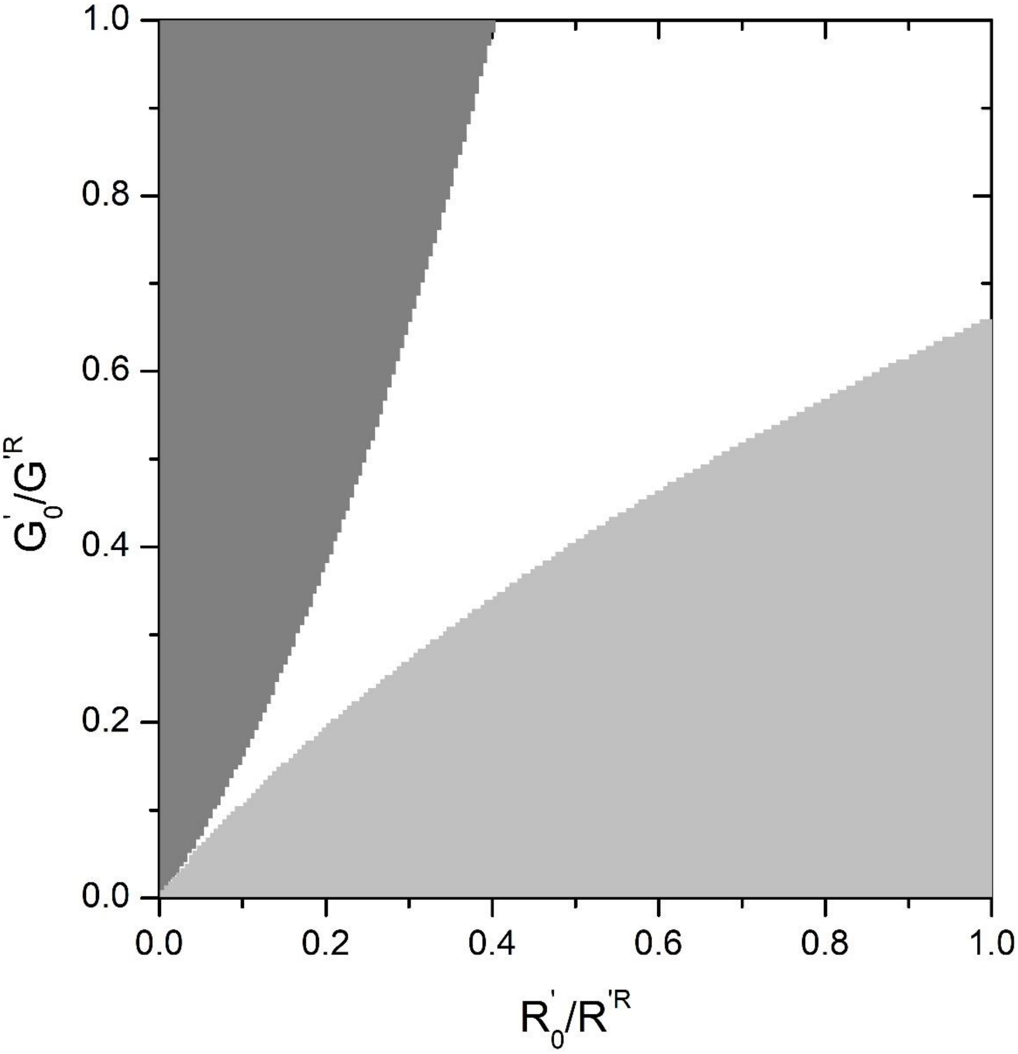

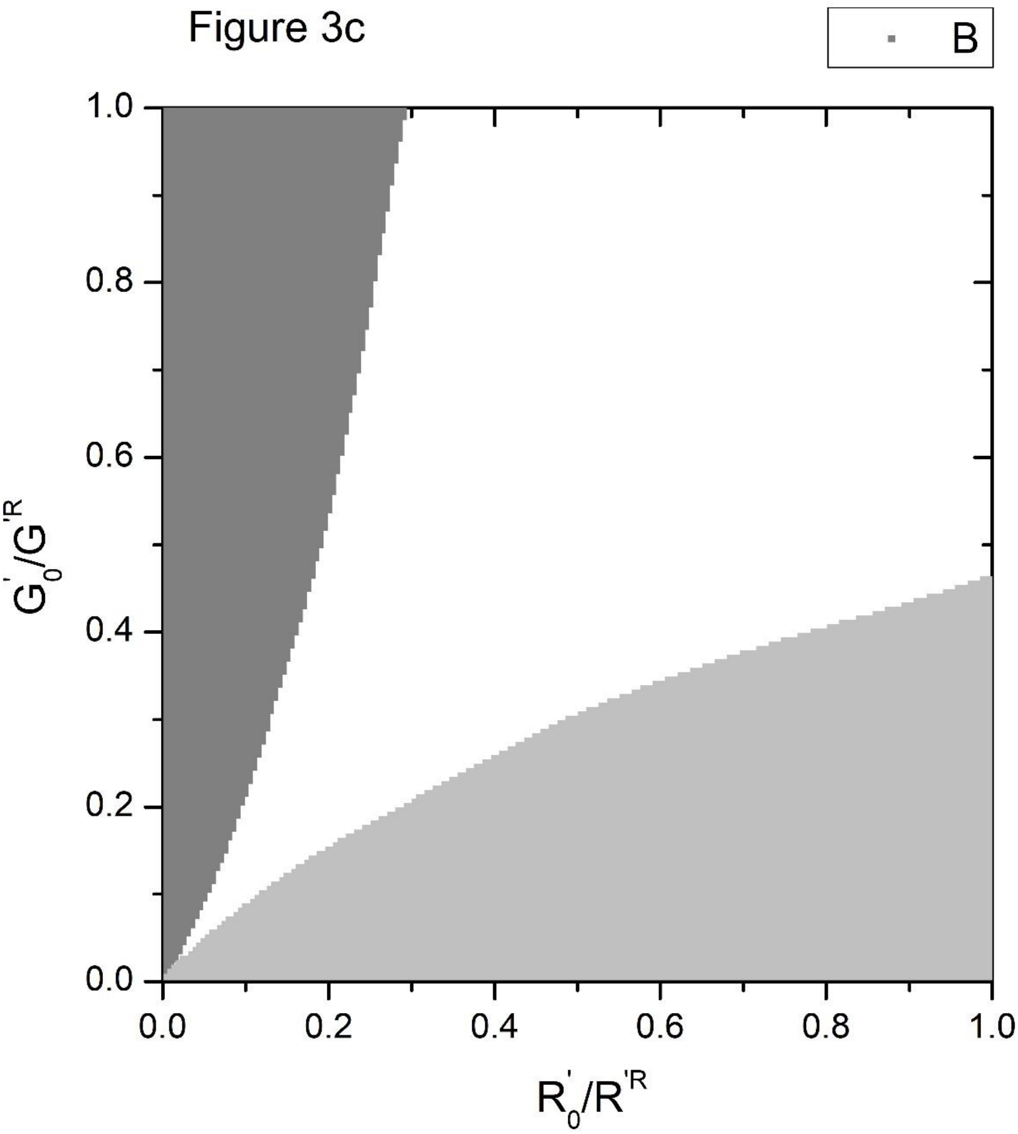

Figure 3c
B
1.0
0.8
0.6
0.4
0.2
0.0
0.0
0.2
0.4
0.6
0.8
1.0
G'0/G'R
R'0/R'R

Figure 3d

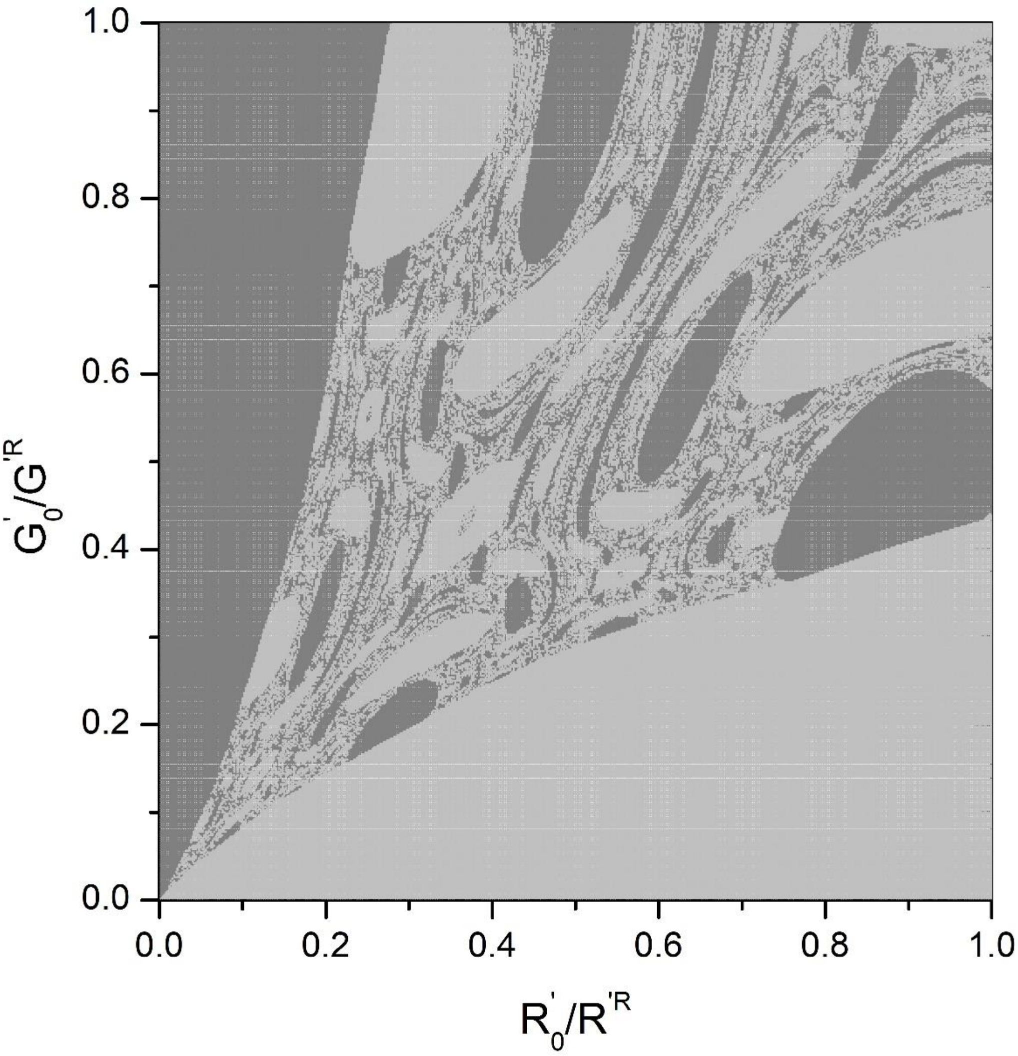

Figure 3e

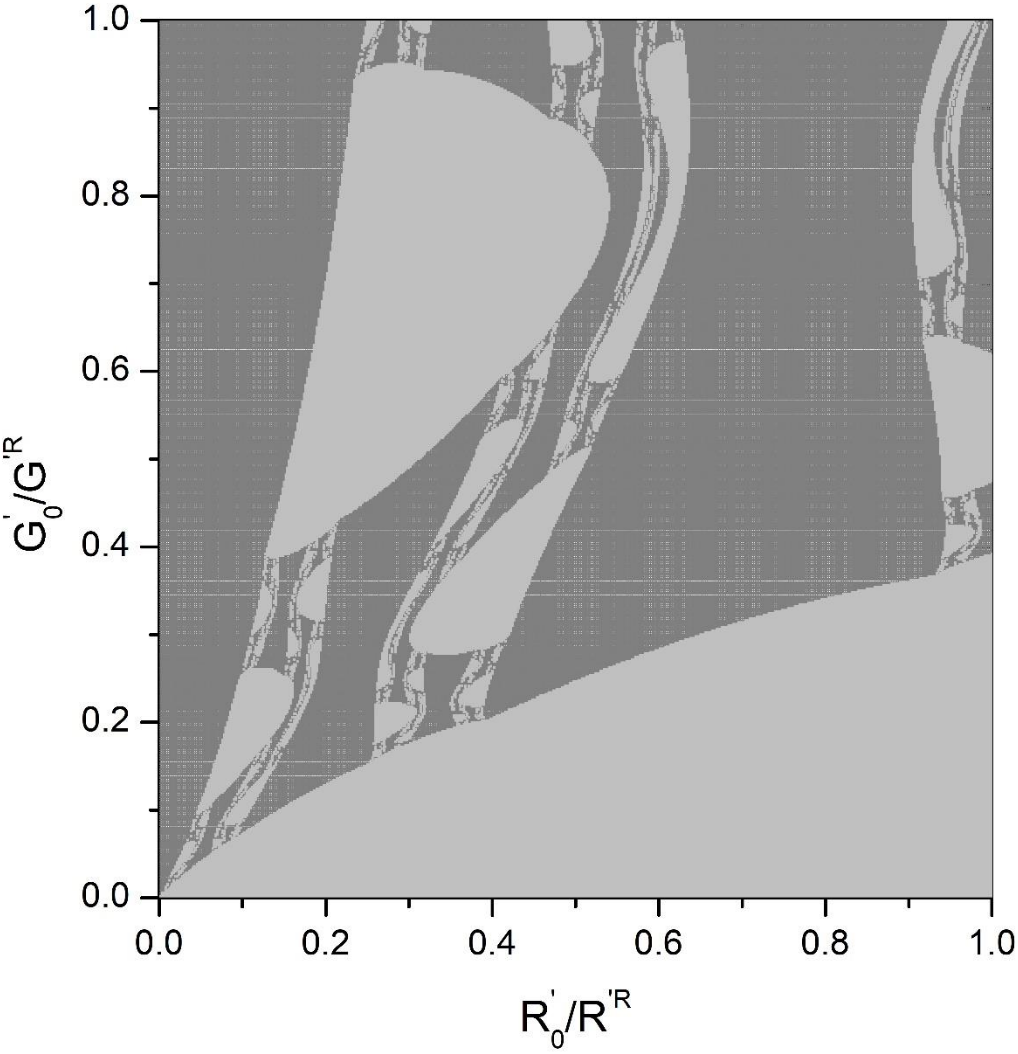

Figure 3f

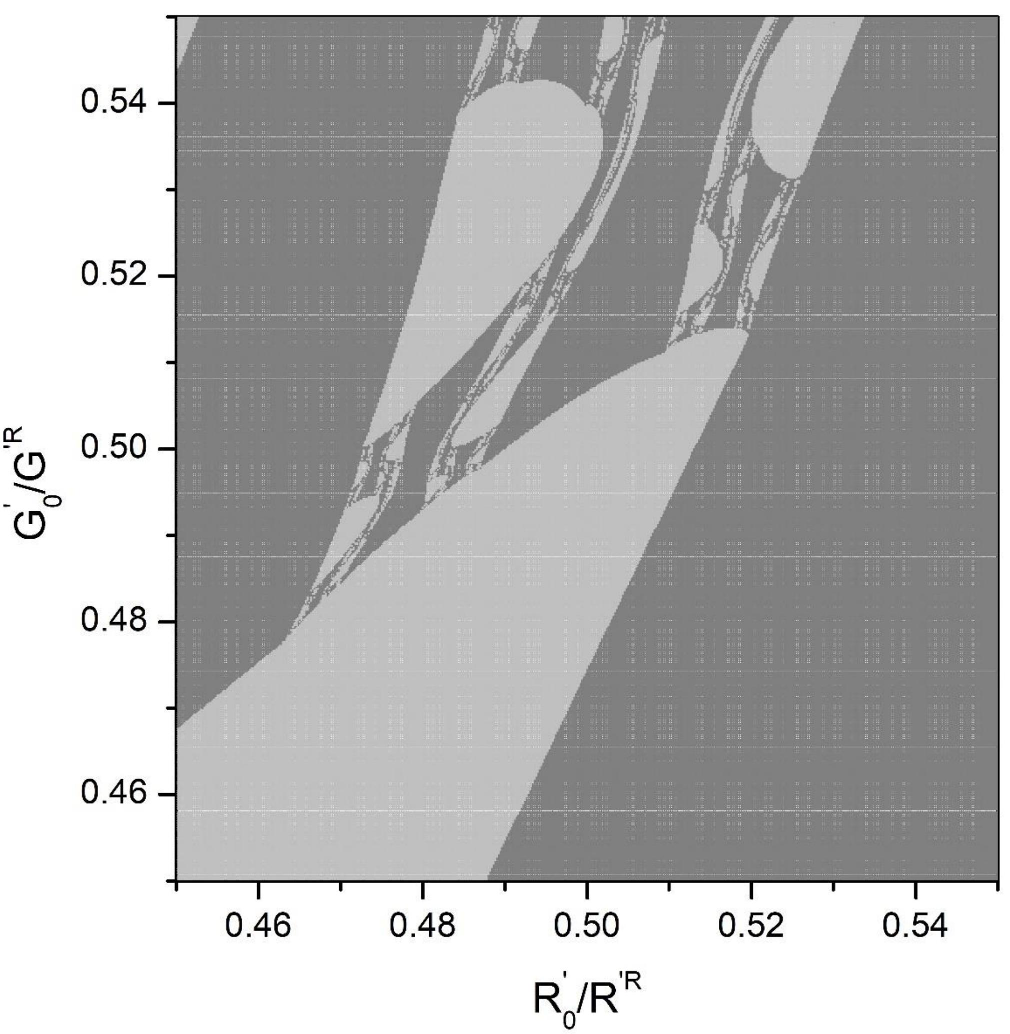

Figure 3g

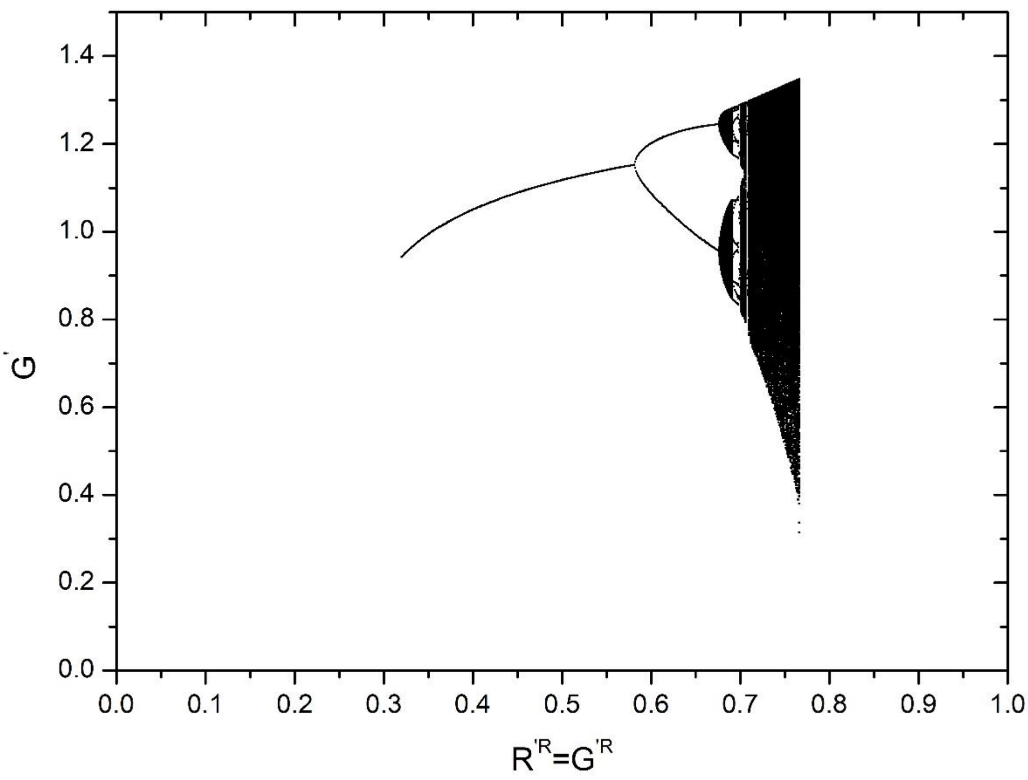

Figure 3h

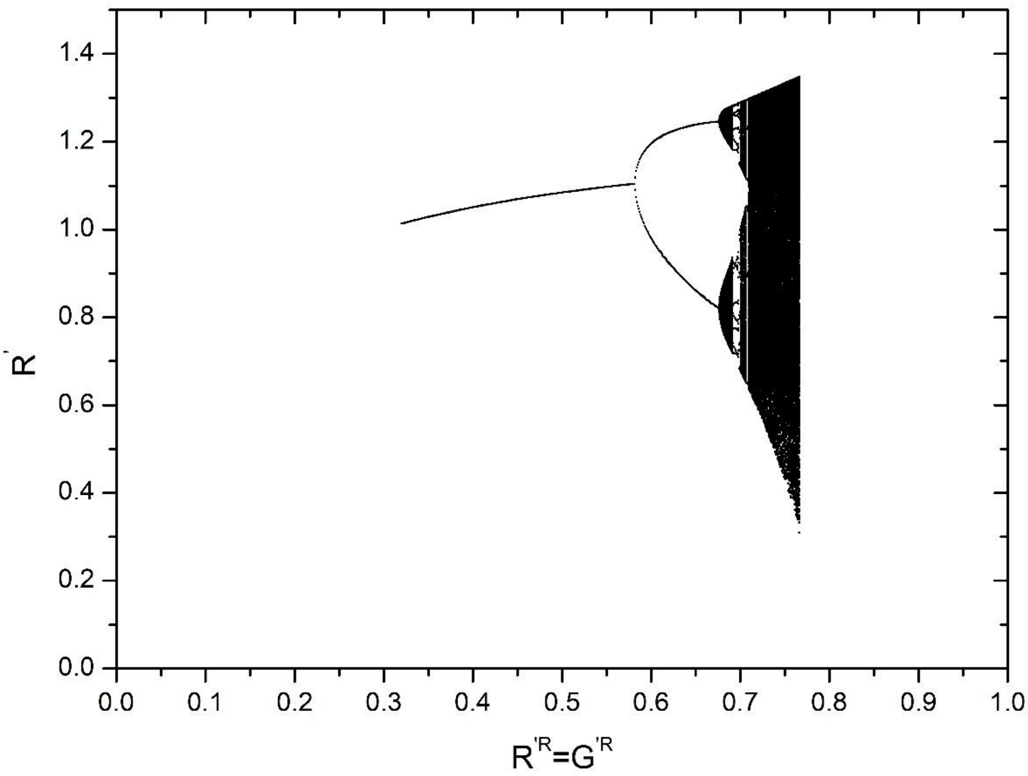

Figure 3i

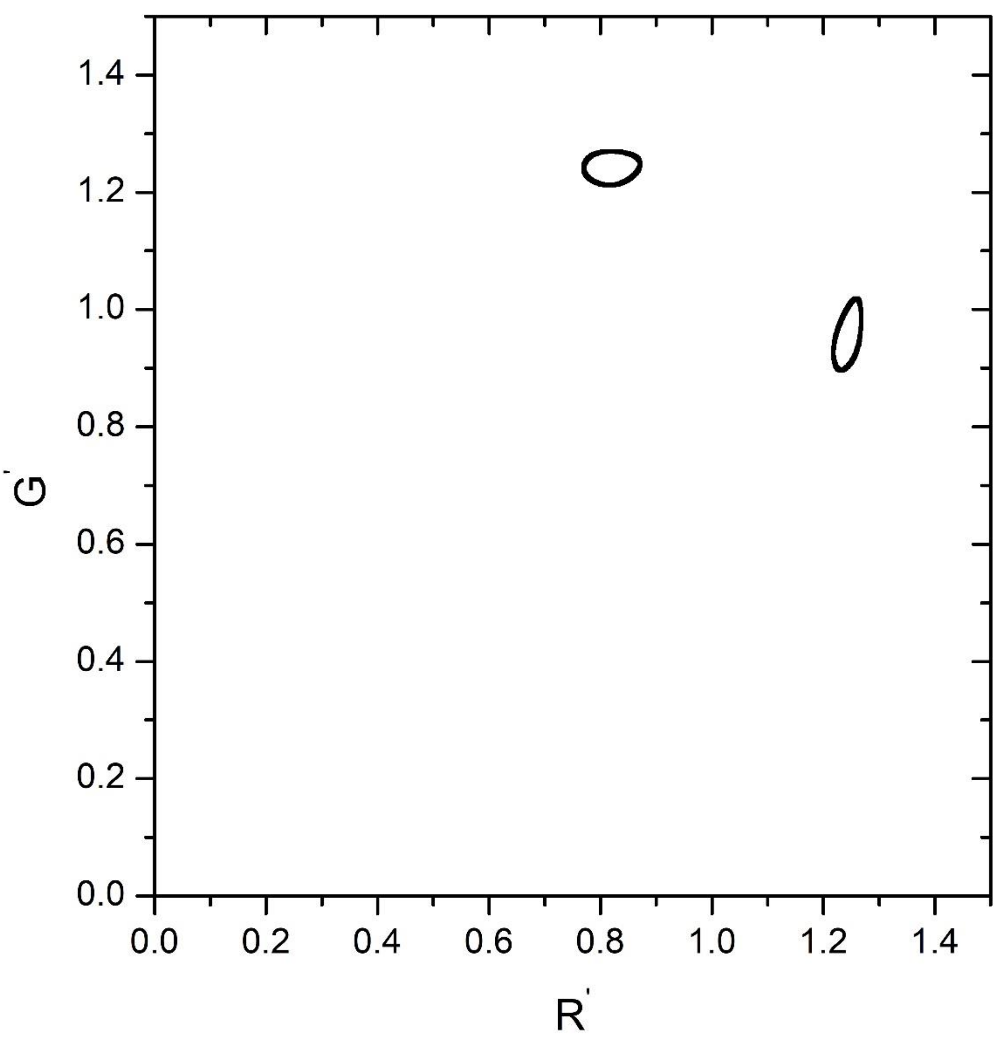

Figure 3j

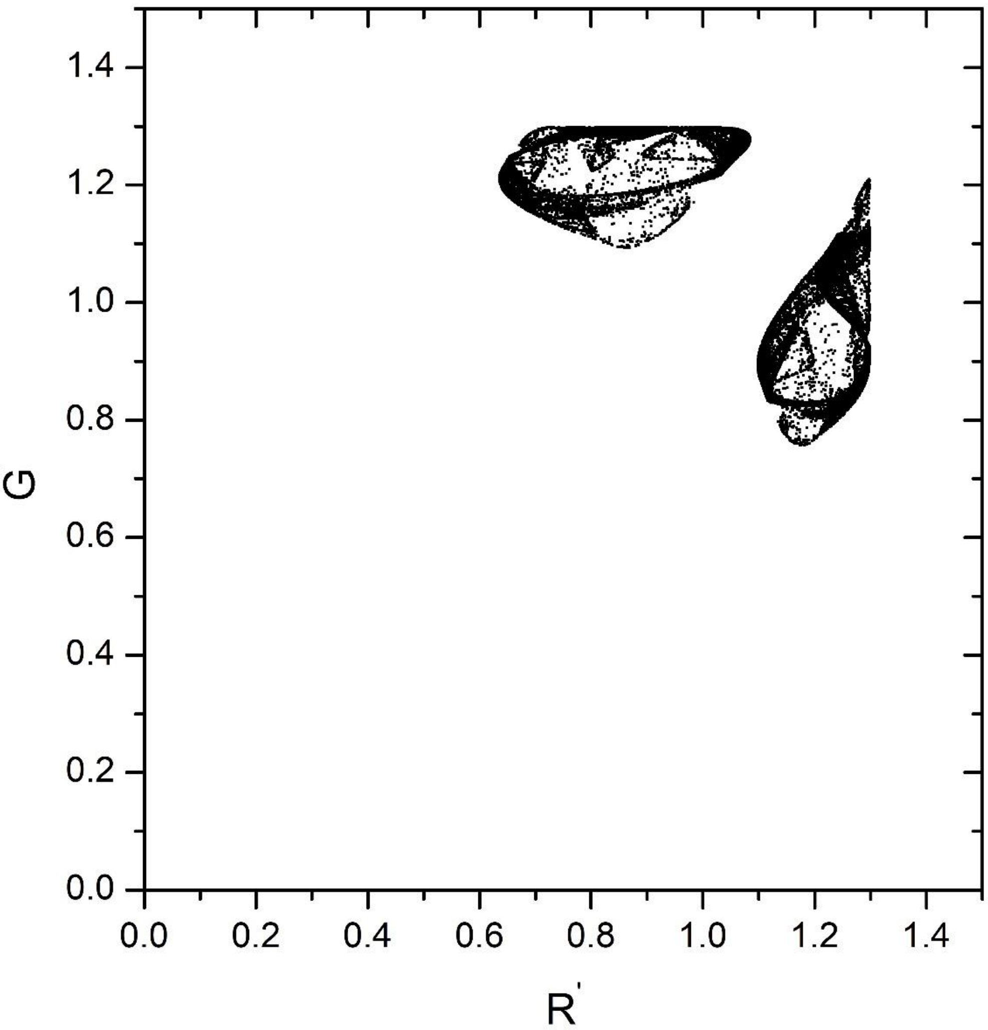

Figure 3k

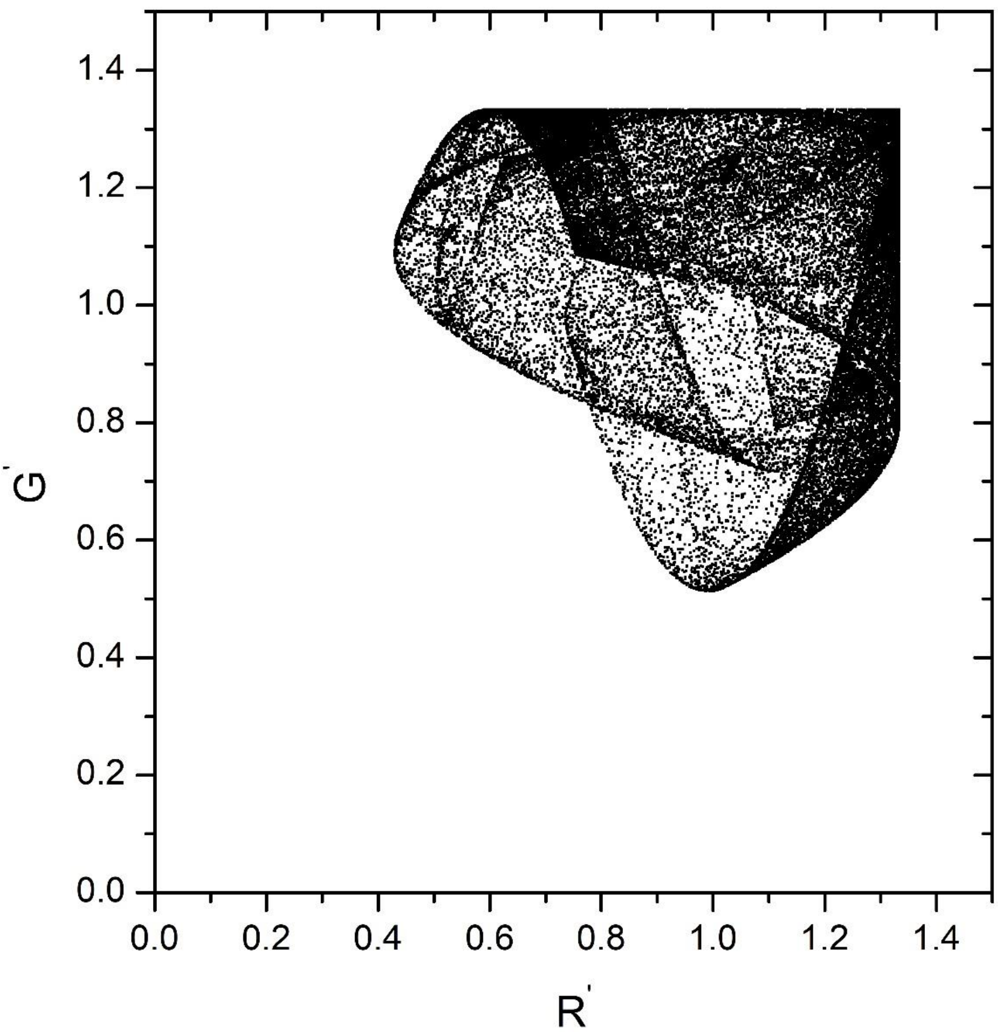

Figure 3 Plots (a-f) illustrate regions of scaled space which lead to victory for Green (grey region) or Red (light grey region). White regions lead to a stalemate. (a) $R^{'R} = G^{'R} = \frac{1}{4}$; (b) $R^{'R} = G^{'R} = \frac{1}{2}$; (c) $R^{'R} = G^{'R} = \frac{3}{4}$ (d); $R^{'R} = G^{'R} = \frac{4}{5}$; (e) $R^{'R} = G^{'R} = 1$; (f) zoom into central region of (e), illustrating the fractal structure; (g) Feigenbaum diagram for G' as $R^{'R} = G^{'R}$ varies over the range [0,1]; (h) Feigenbaum diagram for R' as $R^{'R} = G^{'R}$ varies over the range [0,1]. Plots (i-k) illustrate the behaviour of attractors in the stalemate region of $\left(R^{'}, G^{'}\right)$ space. (i) $R^{'R} = R^{'G} = 0.68$, (j) $R^{'R} = R^{'G} = 0.71$, (k) $R^{'R} = R^{'G} = 0.75$. In all plots $\sqrt{\alpha\beta}\tau = \frac{1}{4}$ and $\xi = \frac{5}{4}$.

Figure 4(a)

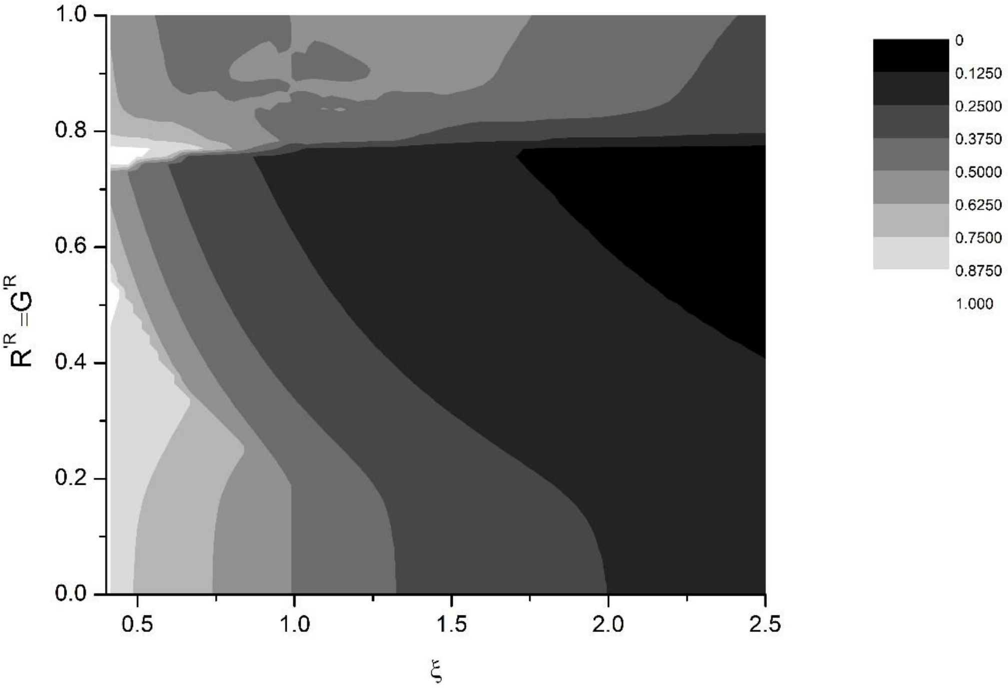

1.0
0.8
0.6
0.4
0.2
0.0
0.5
1.0
1.5
2.0
2.5
$R'^R = G'^R$
ξ
0
0.1250
0.2500
0.3750
0.5000
0.6250
0.7500
0.8750
1.000

Figure 4(b)

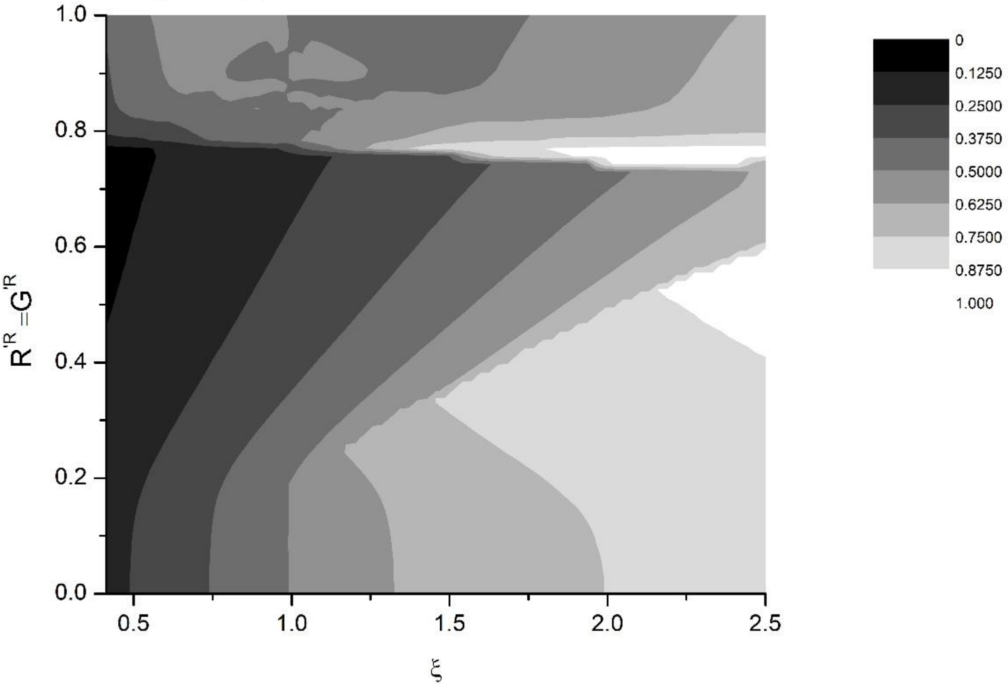

Figure 4(c)

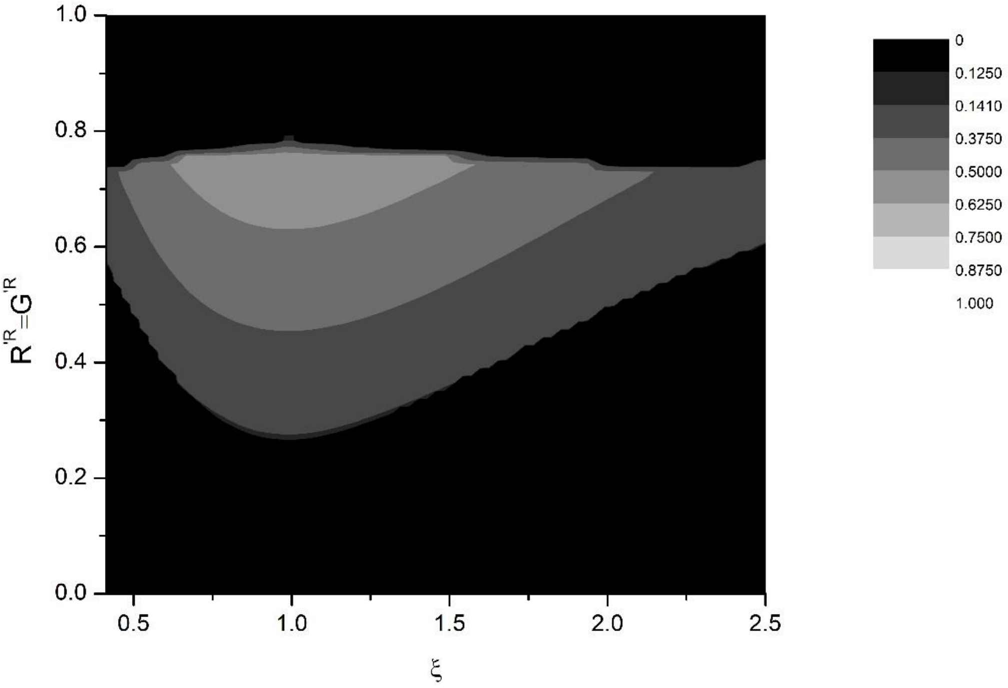

Figure 4 Fractions of $\left(R_0^{'}, G_0^{'}\right)$ space (considered over the range $R_0^{'} \in [0, R^{'R}], G_0^{'} \in [0, G^{'R}]$) which lead to (a) victory for Green; (b) victory for Red; (c) stalemate, as parameters ξ and $R^{'R} = G^{'R}$ are varied. For all figures, $\sqrt{\alpha\beta}\tau = \frac{1}{4}$. Stalemate is assumed if no outright victory has been obtained after 100 battles.

Figure 5 Same as Figure 4 but with $\sqrt{\alpha\beta}\tau = \frac{1}{2}$.

Figure 6 Same as Figure 4 but with $\sqrt{\alpha\beta}\tau = \frac{3}{4}$. Note the change in colour scale in (c).

References

[1] Lanchester F.W. (1916) ‘Aircraft in Warfare: The Dawn of the Fourth Arm’, London: Constable & Co.
[2] Willard D. (1962) ‘Lanchester as a force in history: An analysis of land battles of the years 1618-1905’, Research Analysis Corporation, Bethesda MD, Report No. RAC-TP-74.
[3] Bracken J. (1995) ‘Lanchester Models of the Ardennes Campaign’, Naval Research Logistics, **42(5)**, 559-577.
[4] MacKay N. & Johnson I. (2011) ‘Lanchester models and the battle of Britain’, Naval Research Logistics, **58(3)**, 210-222.
[5] MacKay N., Price C. & Wood A.J. (2016) ‘Weight of Shell Must Tell: A Lanchestrian Reappraisal of the Battle of Jutland’, Journal of the Historical Association, **101**, 536-563.
[6] Clifton E. (2020) ‘A Brief Review on the Application of Lanchester’s Models of Combat in Nonhuman Animals’, Ecological Psychology, **32(4)**, 181-191.
[7] Johnson D.D.P. & MacKay N.J. (2015) ‘Fight the Power: Lanchester’s laws of combat in human evolution’, Evolution & Human Behaviour **36**, 152-163.
[8] Helmhold R.L. (1993) ‘Osipov: The ‘Russian Lanchester’’, European Journal of Operational Research, **65**, 278-288.
[9] Smith D. (1965) ‘The Probability Distribution of the Number of Survivors in a Two-Sided Combat Simulation’, Operational Research Quarterly, **16(4)**, 429-437